# Phosphogypsum stabilization of bauxite residue: Conversion of its alkaline characteristics

Shengguo Xue[1],*, Meng Li[1], Jun Jiang[1], Graeme J. Millar[2], Chuxuan Li[1], Xiangfeng Kong[1]

1. School of Metallurgy and Environment, Central South University, Changsha 410083, China
2. Institute for Future Environments, Science and Engineering Faculty, Queensland University of Technology, Brisbane, Qld 4000, Australia

## ARTICLE INFO

## ABSTRACT

Reduction of the high alkalinity of bauxite residue is a key problem to solve to make it suitable for plant growth and comprehensive utilization. In this study, phosphogypsum, a waste product from the phosphate fertilizer industry, was used to drive the alkaline transformation of the bauxite residue. Under optimal water washing conditions (liquid/solid ratio of 2 mL/g, 30°C, 24 hr), the impact of quantity added, reaction time and reaction mechanism during phosphogypsum application were investigated. Phosphogypsum addition effectively lowered pH levels and reduced the soluble alkalinity by 92.2%. It was found that the concentration of soluble Na and Ca ions in the supernatant increased gradually, whilst the exchangeable $Na^+$ and $Ca^{2+}$ in solid phase changed 112 mg/kg and 259 mg/kg, respectively. $Ca^{2+}$ became the dominant element in the solid phase (phosphogypsum addition of 2%, liquid/solid ratio of 2 mL/g, 30°C, 12 hr). X-ray diffraction data indicated that cancrinite and hydrogarnet were the primary alkaline minerals. SEM images suggested that phosphogypsum could promote the formation of stable macro-aggregates, whilst the content of $Ca^{2+}$ increased from 5.6% to 18.2% and Na reduced from 6.8% to 2.4%. Treatment with phosphogypsum could significantly promote the transformation of alkalinity cations by neutralization, precipitation and replacement reactions. This research provided a feasible method to promote soil formation of bauxite residue by phosphogypsum amendment.

## Introduction

The rapid development of the alumina industry in recent years has brought about a series of environmental problems (Chen et al., 2017; Wu et al., 2016), which have restricted sustainable development (Gelencsér et al., 2011; Mayes et al., 2016). Aluminum processing, results in a by-product described as bauxite residue (BR) which is separated into red mud and red sand according to particle size between different refineries. These materials differ in terms of both physical and chemical properties (Xu et al., 2018). Approximately 150 million tons of BR are produced per year by the extraction of alumina using the Bayer process. Moreover, the global inventory of red mud was in excess of 4 billion tons in 2015 (Xue et al., 2016a; Zhu et al., 2015). China is a major producer of alumina and about 61 million tons of BR was generated in 2016 (Zhu et al., 2016b).
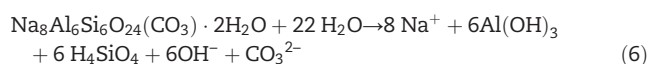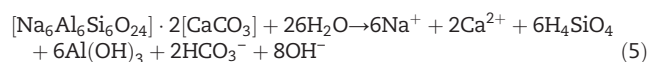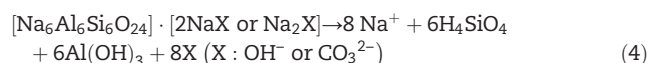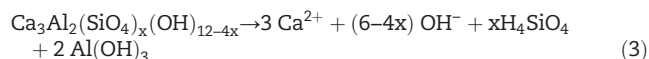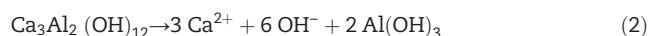
Therefore, the development of strategies to effectively manage BR and protect the environment has become more important (Lockwood et al., 2015; Xue et al., 2018). At present,
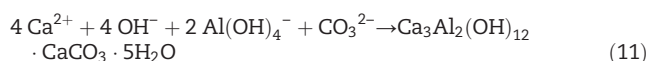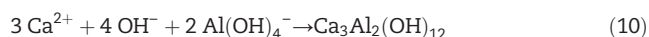
BR is mainly large-scale stored on land adjacent to the alumina refineries to form the bauxite residue disposal area (BRDA) (Zhu et al., 2016c; Kong et al., 2018a). Due to the significant moisture content of BR, there are serious environmental safety risks in BRDA, such as tailings dam failure and landslide risks. High alkalinity leachates of BR present challenges for the management of BRDAs. For example, constructed wetlands planted with *Phragmites australis* were one approach demonstrated to effectively treat alkaline bauxite-residue leachate (Higgins et al., 2016, 2017). Trace metals are also present in BR which can cause hazardous environmental situations due to their mobility (Lockwood et al., 2015). Another major concern is fugitive dust which is generated from BR and potentially results in harm to surrounding communities (Xu et al., 2018). Collectively, these outlined problems make it difficult to remediate and establish a vegetation cover in a BRDA (Courtney and Mullen, 2009). In order to effectively manage BRDA, strategies which could convert this material into a soil-like medium by revegetation, are regarded as the most promising prospect (Zhu et al., 2018).

Extraction of alumina content from the Bayer process results in a highly alkaline by-product with inherently variable physical and chemical properties (Kong et al., 2017a; Santini et al., 2015; Xue et al., 2016b; Zhu et al., 2016a). The alkali components of BR are complex and generally can be divided into two categories: soluble alkali and chemical bonded alkali (Kong et al., 2017b). The soluble alkali component mainly includes sodium hydroxide (NaOH), sodium carbonate ($Na_2CO_3$), sodium bicarbonate ($NaHCO_3$), sodium aluminate ($NaAl(OH)_4$), sodium silicate ($Na_2SiO_3$), potassium hydroxide (KOH), and potassium carbonate ($K_2CO_3$). These alkaline anions ($OH^-$, $Al(OH)_4^-$, $CO_3^{2-}$, $HCO_3^-$) were resolved by soluble alkali, which are the primary alkalinity anions in BR. Removing these anions can significantly reduce the pH of BR (Clark et al., 2015; Kinnarinen et al., 2015). In contrast, chemical bonded alkalis, such as calcite ($CaCO_3$), sodalite ($[Na_6Al_6Si6O_{24}]\cdot[2NaX$ or $Na_2X]$), cancrinite ($[Na_6Al_6Si_6O_{24}]\cdot2[CaCO_3]$), hydrogarnet ($Ca_3Al_2(SiO4)_x(OH)_{12-4x}$) and tricalcium aluminate (TCA, $Ca_3Al_2(OH)_{12}$) are relatively stable and exhibit low solubility. The dissolution reactions of these species can occur as shown in Eqs. (1) to (6) (Higgins et al., 2017; Paradis et al., 2007; Radomirovic et al., 2013; Santini et al., 2011; Whittington et al., 1998).

$$CaCO_3 \rightarrow Ca^{2+} + CO_3^{2-} \tag{1}$$

$$Ca_3Al_2(OH)_{12} \rightarrow 3\,Ca^{2+} + 6\,OH^- + 2\,Al(OH)_3 \tag{2}$$

$$Ca_3Al_2(SiO_4)_x(OH)_{12-4x} \rightarrow 3\,Ca^{2+} + (6{-}4x)\,OH^- + xH_4SiO_4 + 2\,Al(OH)_3 \tag{3}$$

$$[Na_6Al_6Si_6O_{24}]\cdot[2NaX \text{ or } Na_2X] \rightarrow 8\,Na^+ + 6H_4SiO_4 + 6Al(OH)_3 + 8X\ (X:OH^- \text{ or } CO_3^{2-}) \tag{4}$$

$$[Na_6Al_6Si_6O_{24}]\cdot2[CaCO_3] + 26H_2O \rightarrow 6Na^+ + 2Ca^{2+} + 6H_4SiO_4 + 6Al(OH)_3 + 2HCO_3^- + 8OH^- \tag{5}$$

$$Na_8Al_6Si_6O_{24}(CO_3)\cdot2H_2O + 22\,H_2O \rightarrow 8\,Na^+ + 6Al(OH)_3 + 6\,H_4SiO_4 + 6OH^- + CO_3^{2-} \tag{6}$$

Therefore, a combination of high concentrations of alkalinity, significant salinity, low microbial activity, Na content and reduced nutrient retention limit plant growth and thus comprehensive utilization with BR. To solve the aforementioned problems with BR stockpiling, considerable research effort has been devoted towards de-alkalization of BR. However, most of the suggested technical solutions cannot be implemented on a large scale. Use of inorganic acid neutralization, acidic gas neutralization, gypsum, seawater and brine have been popularized (Couperthwaite et al., 2014; Courtney and Kirwan, 2012; Dilmore et al., 2008; Kirwan et al., 2013; Lehoux et al., 2013; Menzies et al., 2004; Rai et al., 2013). Neutralization, precipitation and inhibition effects are observed in the process of ecological disposal and these reaction mechanisms are used to control the alkalinity in BR. The gypsum method produces less secondary pollutants, during *in situ* restoration of BRDA. Gypsum can continuously provide $Ca^{2+}$ which reacts with $CO_3^{2-}$, $HCO_3^-$, $OH^-$ and $Al(OH)_4^-$ to generate calcite, calcium hydroxide and tricalcium aluminate etc. (Eqs. (7)–(11)).

$$H^+ + OH^- \rightarrow H_2O \tag{7}$$

$$Ca^{2+} + 2\,OH^- \rightarrow 2Ca(OH)_2 \tag{8}$$

$$Ca^{2+} + CO_3^{2-} \rightarrow CaCO_3 \tag{9}$$

$$3\,Ca^{2+} + 4\,OH^- + 2\,Al(OH)_4^- \rightarrow Ca_3Al_2(OH)_{12} \tag{10}$$

$$4\,Ca^{2+} + 4\,OH^- + 2\,Al(OH)_4^- + CO_3^{2-} \rightarrow Ca_3Al_2(OH)_{12} \cdot CaCO_3 \cdot 5H_2O \tag{11}$$

Ideally, treatment of BR should best be conducted using a low cost approach due to the vast amount of material present. Therefore, application of a waste material to solve this issue is a potentially attractive strategy. Notably, during the processing of phosphate rocks by sulfuric acid to obtain fertilizer, a residue termed phosphogypsum is produced. This material has increasingly been considered as a resource in recent years and not simply as a waste (Cánovas et al., 2017a). For example, Cánovas et al. (2017b) discussed the viability of recovering rare earth materials from phosphogypsum. Additionally, researchers have utilized phosphogypsum as an amendment to decrease pH in BR (Jones et al., 2012; Singh and Garg, 2005). The release of $Ca^{2+}$ ions into solution is a key factor when amending BR with phosphogypsum, due to the ability of these species to neutralize and precipitate soluble alkali cations. However, the soluble alkalinity itself can leach under certain conditions. Thus these methods still have some shortcomings: for example, the effect of the leaching rate and time of BR alkaline, these certain conditions were very important for the amendment of phosphogypsum treatment.

Therefore, the aim of this short-term study was to examine the control of alkalinity in BR using phosphogypsum addition. The hypothesis was that phosphogypsum would behave similarly to gypsum and allow an economic means of remediating bauxite residue. Specific research questions included: What is the impact of contact time when phosphogypsum is reacted with BR? How does the amount of phosphogypsum present influence the reaction with BR? And, what mineral phases and morphological changes occur in the bauxite residue upon reaction with phosphogypsum amendment. To answer the aforementioned research questions, bench scale tests were conducted with the BR and phosphogypsum generated in China.

# 1. Materials and methods

## 1.1. Materials

The raw BR sample used in this study was collected from the Pingguo Refinery operated by the Aluminum Corporation of China Limited, Guangxi Province, China. Raw phosphogypsum was collected from Yunnan Province. Samples were thoroughly homogenized and dried at 65°C for 72 hr. Subsequently, samples were ground into a fine powder using a mortar and pestle and sieved (100 mesh, mesh aperture is 150 μm).

## 1.2. Methods

The water leaching behavior of BR was firstly carried out to ascertain the optimum conditions (liquid/solid ratio 2, temperature 30°C and time 24 hr) (Li et al., 2018). Under the optimum conditions of water leaching, the control of alkalinity in BR was carried out using phosphogypsum. In view of the economy and efficiency, a single-factor experiment was used to assess the stabilization effect of phosphogypsum including quantity added and reaction time. The ratio (wt.%) of added phosphogypsum was set as 0.5% (0.1 g), 1% (0.2 g), 1.5% (0.3 g), 2% (0.4 g), 3% (0.6 g), 4% (0.8 g), and 5% (1.0 g) with 20 g BR sample, while the reaction time was controlled at 1, 2, 4, 8, 12, 18, and 24 hr with 2% (0.4 g) phosphogypsum and 20 g BR sample. Three replicates of each treatment were completed in order to effectively reduce the error. Weighed BR sample (20 g) was mixed with phosphogypsum and 40 mL deionized water in 250 mL bottles. Subsequently, the mixed slurry was stirred sufficiently for 30 sec and sealed with a plastic membrane to prevent external interference. The experimental temperature was controlled by a water bath, and SHZ-D (III) vacuum suction filters were used to filter leachate. Filter residue was naturally dried and extracted supernatant with ammonium acetate.

## 1.3. Chemical analysis

EC (electrical conductivity) and pH were measured by a PHS-3C pH meter and a DDS-307 conductivity meter, respectively (Johnston et al., 2010). The supernatant extracted by ammonium acetate (pH = 7) was used to evaluate exchangeable $Ca^{2+}$, $Mg^{2+}$, $K^+$, $Na^+$, and $Al^{3+}$ ions. These exchangeable and soluble cations in the supernatant were analyzed by inductively coupled plasma atomic emission spectroscopy (ICP-AES) (Huang et al., 2016). Carbonate ($CO_3^{2-}$) and bicarbonate ($HCO_3^-$) were assessed by double indicator-neutralization titration using $H_2SO_4$ (0.005 mol/L).

## 1.4. Mineral phase and morphological analysis

Raw BR sample and residue solids (0.04–0.05 mm) were characterized by X-ray powder diffraction (XRD). XRD was conducted with a 2θ scan range from 10 to 80° at a step size of 1°/sec. Patterns were indexed using Jade6. Sample morphology was of 0.1–0.05 mm grains was achieved with a scanning electron microscope equipped with energy dispersive X-ray spectroscopy (Newson et al., 2006).

## 1.5. Data analysis

All data were analyzed in Microsoft Office Excel 2010 and IBM SPSS Statistics 20. All of the figures were constructed by Origin Pro8.0.

# 2. Results and discussion

## 2.1. Effect of phosphogypsum quantity on bauxite residue

The effect of phosphogypsum amendments on the alkalinity, pH, and concentration of soluble anions in the supernatant is presented in Table 1 (L/S ratio of 2 mL/g, 30°C, 24 hr). Due to the existence of a variety of alkaline species (NaOH, $Na_2CO_3$, $NaHCO_3$, $NaAl(OH)_4$), the pH of the fresh samples was in the range 10 to 11, and the average pH was 10.6. The pH of BR showed a significant reduction with the addition of phosphogypsum, and the final pH of the processed sample was approximately 8.1. Several researchers have examined application of phosphogypsum to alkaline materials (Singh and Garg, 2005) and noted pH was reduced after gypsum utilization to BR (Courtney and Timpson, 2005; Lee et al., 2007; Lehoux et al., 2013). It has been suggested that an excess of soluble calcium in the form of gypsum can reduce pH to levels suited to plant growth by precipitating soluble alkalinity and suppressing the solubility of solid phase alkalinity (Courtney

**Table 1 – pH, electrical conductivity, alkalinity anions for the supernatants of bauxite residue amended with phosphogypsum.**

| Parameters | Phosphogypsum | | | | | | | |
|---|---|---|---|---|---|---|---|---|
| | 0 | 0.5% | 1% | 1.5% | 2% | 3% | 4% | 5% |
| pH | 10.6 ± 0.86[a] | 10.3 ± 0.40[a] | 10.1 ± 0.37[a] | 8.8 ± 0.45[b] | 8.1 ± 0.11[b] | 8.1 ± 0.24[b] | 8.2 ± 0.21[b] | 8.2 ± 0.29[b] |
| EC (mS/cm) | 2.1 ± 0.24[f] | 5.2 ± 0.55[e] | 5.5 ± 0.35[d] | 6.0 ± 0.56[c] | 6.4 ± 0.44[b] | 6.6 ± 0.07[a,b] | 6.6 ± 0.10[a] | 6.6 ± 0.05[a] |
| $c(OH^-)$ (mmol/L) | <0.001 | <0.001 | <0.001 | <0.001 | <0.001 | <0.001 | <0.001 | <0.001 |
| $c(CO_3^{2-})$ (mmol/L) | 37.2 ± 1.26[a] | 27.2 ± 2.06[b] | 8.4 ± 0.25[c] | 1.0 ± 0.25[d] | 0.2 ± 0.01[d] | 0.2 ± 0.01[d] | 0.2 ± 0.01[d] | 0.2 ± 0.01[d] |
| $c(HCO_3^-)$ (mmol/L) | 14.5 ± 0.38[a] | 13.2 ± 0.64[a] | 10.3 ± 1.14[b] | 5.5 ± 1.12[c] | 3.9 ± 0.10[c] | 4.3 ± 0.45[c] | 4.4 ± 0.55[c] | 4.1 ± 0.38[c] |
| $c(Al(OH)_4^-)$ (mmol/L) | 1.1 ± 0.02[a] | 1.0 ± 0.01[b] | 0.4 ± 0.06[c] | 0.04 ± 0.01[d] | 0.02 ± 0.01[d] | 0.02 ± 0.01[d] | 0.02 ± 0.01[d] | 0.02 ± 0.01[d] |
| Alkalinity* (mmol/L) | 52.8 ± 1.21[a] | 41.4 ± 1.93[b] | 19.2 ± 0.88[c] | 6.5 ± 1.37[d] | 4.1 ± 0.10[d] | 4.5 ± 0.46[d] | 4.6 ± 0.55[d] | 4.3 ± 0.38[d] |

Different letters of the same line indicate significant differences in the addition of different phosphogypsum ($p < 0.05$).
* Soluble alkalinity = $c(OH^-) + c(CO_3^{2-}) + c(HCO_3^-) + c(Al(OH)_4^-)$.

and Kirwan, 2012). The EC was 6.6 mS/cm when phosphogypsum dosage was 3%–5% (0.6–1.0 g), which probably reflected changes in the $Na^+$ and $Ca^{2+}$ concentrations. In particular, the phosphogypsum released soluble $Ca^{2+}$ into solution and promoted precipitation of soluble alkaline anions; which caused significant increase in EC. Support for this conclusion was gained from the fact that gypsum amended residue had EC values ranging from 2.1–4.5 mS /cm with higher levels recorded and $Ca^{2+}$ was the major soluble ion in the gypsum amended process (Courtney and Mullen, 2009).

When 2% of phosphogypsum was added, the anion concentration of $CO_3^{2-}$, $HCO_3^-$ and $Al(OH)_4^-$ reduced to the lowest value: 0.2 mmol/L, 3.9 mmol/L and 0.02 mmol/L, respectively. This result suggested that soluble alkalinity of BR decreased to 92.2% and thus high soluble alkalinity concentration effects were mitigated. Application of gypsum (0, 40 and 90 ton/ha) reduced sodicity and promoted nutrient uptake for P and Mn, which was indispensable for plant growth (Courtney and Harrington, 2012). When the ratio of phosphogypsum continuously increased, the alkaline anion concentration began to decrease slowly and then remained steady for the duration of the exposure period. According to Table 1, among these alkaline anions, the concentration of $CO_3^{2-}$ exhibited the greatest decrease and it was the dominant component of soluble alkali anion. The content of $Al(OH)_4^-$ was minimal because most aluminum was insoluble and crystallized. As Jones et al. (2015) reported, $Ca^{2+}$ could react with soluble alkaline anions such as $CO_3^{2-}$, $HCO_3^-$, $OH^-$ and $Al(OH)_4^-$. The mechanisms of both gypsum and phosphogypsum were similar, as both materials can provide excess calcium to precipitate soluble alkali (Kopittke et al., 2005; Jones et al., 2012). Notably, phosphogypsum dissolution released not only substantial divalent calcium but also some hydrogen ions, which consumed soluble alkalinity to precipitate calcium carbonate.

The measured concentration of cations indicated that most substances were insoluble and existed in crystalline form (Table 2). Initially there was an increase of soluble sodium concentration which gradually stabilized at 83 mmol/L when the addition of phosphogypsum was 2%. Soluble calcium had an original concentration of 0.04 mmol/L, and increased to approximately 10 mmol/L. On the contrary, the concentrations of soluble potassium and magnesium were almost impervious ($p > 0.05$). Addition of phosphogypsum resulted in precipitation of $CaCO_3$ to release soluble sodium. Gobran and Miyamoto (1985) suggested that increasing salt concentration could promote gypsum dissolution, which was similar to the behavior of phosphogypsum dissolution. In a BR slurry, phosphogypsum dissolution observably increased and

released abundant soluble calcium. The addition of a calcium source, most of them would react with the soluble alkalis and precipitate $CaCO_3$ to significantly drive the pH and some of them would remain in the supernatant to increased excess calcium. As calcium was released, alkaline carbonate in the BR was precipitated due to $CaCO_3$ formation (which was insoluble in alkaline solution).

The concentration of exchangeable $Na^+$ reduced to 112 mg/kg by the addition of phosphogypsum, while the concentration of exchangeable $Ca^{2+}$ was concomitantly increased. When the addition of phosphogypsum was 2%, the amount of $Na^+$ and $Ca^{2+}$ had significant differences ($p < 0.05$) compared with other treatments (Fig. 1). Co-application of spent mushroom compost and gypsum could reduce the values of exchangeable $Na^+$ to below 10% which might benefit for plant growth (Courtney and Harrington, 2012). However, concentrations of exchangeable $K^+$ and $Mg^{2+}$ were mostly unaffected by addition of phosphogypsum ($p > 0.05$). The abundance of exchangeable cations in initial BR slurry was in the order: $Na^+ > Ca^{2+} > K^+ > Mg^{2+}$. The initial content of $Ca^{2+}$ increased to 259 mg/kg, which meant that calcium became the dominant element in the residue.

Concentrations of exchangeable $Na^+$ were lowered during phosphogypsum treatment. The reason for this effect was that $Na^+$ was a monovalent cation and was not sorbed strongly on the cation exchange sites (Jones et al., 2015). The primary sodium salts (NaOH, $Na_2CO_3$, $NaHCO_3$, $NaAl(OH)_4$) were able to leach soluble alkalinity ($CO_3^{2-}/HCO_3^-$) and promote alkaline reduction (Kong et al., 2018b). Leaching of significant amounts of divalent $Ca^{2+}$ indicated that soluble sodium ions in BR were replaced by calcium. Phosphogypsum amendment produced a lower exchangeable $Na^+$ concentration and higher exchangeable $Ca^{2+}$ content with 2% phosphogypsum application in the solid residue.

From what has been discussed above, 2% of phosphogypsum is preferred. In this case, the pH and soluble alkalinity were considerably lower, whilst the content of soluble sodium was increased. This change indicated that the main soluble alkali species in BR (NaOH, $Na_2CO_3$, $NaHCO_3$ and $NaAl(OH)_4$) were continuously dissolved to release ions and reduce alkalinity.

## 2.2. Effect of contact time upon interaction of phosphogypsum and bauxite residue

The impact of reaction time upon the concentration of alkaline ions and pH of the supernatant was evaluated with phosphogypsum addition of 2%, L/S ratio of 2 mL/g, and temperature of 30°C.

**Table 2 – Soluble cation ($Na^+$, $Ca^{2+}$, $Mg^{2+}$, $K^+$) for the supernatants of bauxite residue amended with phosphogypsum.**

| Soluble cation | Phosphogypsum | | | | | | | |
|---|---|---|---|---|---|---|---|---|
| | 0 | 0.5% | 1% | 1.5% | 2% | 3% | 4% | 5% |
| c($Na^+$) (mmol/L) | 54.1 ± 0.85[d] | 66.3 ± 1.95[c] | 63.6 ± 2.53[c] | 78.7 ± 0.38[b] | 83.0 ± 1.05[a] | 84.2 ± 0.67[a] | 80.7 ± 0.20[ab] | 82.0 ± 1.31[ab] |
| c($K^+$) (mmol/L) | 4.2 ± 0.25[ab] | 4.1 ± 0.36[b] | 4.0 ± 0.40[b] | 4.2 ± 0.19[ab] | 4.6 ± 0.04[ab] | 4.8 ± 0.34[a] | 4.6 ± 0.15[ab] | 4.7 ± 0.11[ab] |
| c($Ca^{2+}$) (mmol/L) | 0.04 ± 0.01[c] | 0.05 ± 0.01[c] | 0.04 ± 0.01[c] | 0.54 ± 0.05[c] | 7.0 ± 0.85[b] | 10.4 ± 0.07[a] | 10.5 ± 0.14[a] | 10.6 ± 0.17[a] |
| c($Mg^{2+}$) (mmol/L) | 0.03 ± 0.01[b] | 0.04 ± 0.01[b] | 0.02 ± 0.01[b] | 0.02 ± 0.01[b] | 0.04 ± 0.01[ab] | 0.06 ± 0.01[ab] | 0.07 ± 0.01[a] | 0.05 ± 0.01[ab] |

Different letters of the same line indicate significant differences in the addition of different phosphogypsum ($p < 0.05$).
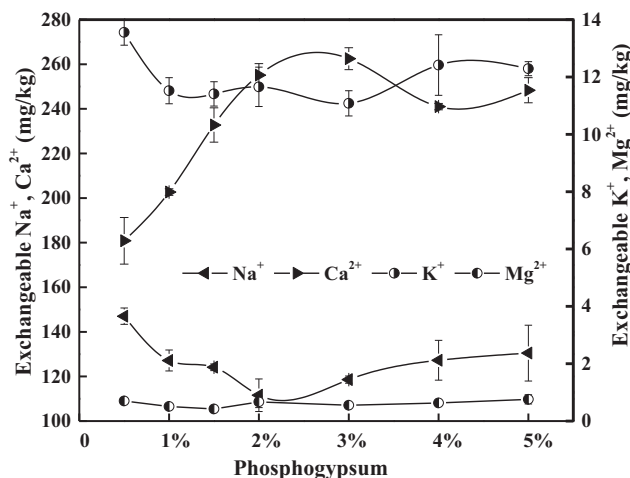
**Fig. 1 – Effect of phosphogypsum addition on exchangeable cations of bauxite residue.**

The pH of supernatant was controlled in the range from 8.1 to 7.7 over a 12 hr period. The concentration of $CO_3^{2-}$ (0.7 to 0.2 mmol/L) and $HCO_3^-$ (5.2 to 3.3 mmol/L) were reduced and maintained for the duration of the exposure period. The range of pH was slightly only slightly changed by the reaction time ($p > 0.05$). However, there was greater variance in the soluble cations ($Na^+$ and $Ca^{2+}$), which were released from 62 to 86 mmol/L and 5.5 to 8.3 mmol/L, respectively (Fig. 2).

Kopittke et al. (2005) suggested that gypsum dissolution was an ionic transport-controlled process, which typically involved $Ca^{2+}$ transfer into solution at a fast rate. With gypsum application, $OH^-$ and $CO_3^{2-}$ firstly took part in neutralization reaction and precipitated calcite within a relatively short time (12 hr). The addition of calcium promoted the release of sodium ions that potentially reduced salt stress to plant growth. High alkalinity and salinity are critical factors that can hinder soil formation and seedling emergence. Excess salts inhibit seedling germination, which reduces the BR water potential (Courtney and Kirwan, 2012). When

increasing stabilization time, the concentration of calcium ions didn't increase substantially in the supernatant of BR reminded with phosphogypsum. An important aspect was the presence of $CaSO_4 \cdot H_2O$ in phosphogypsum, which had different solubility due to limitations associated with the surface solution concentrations of $Ca^{2+}$ and $SO_4^{2-}$. During phosphogypsum amendment for different time periods, concentration of soluble potassium and magnesium was only marginally lower. The concentrations of soluble sodium and calcium were in a dynamic equilibrium state after 12 hr.

The effect of reaction time on changes in exchangeable cations ($Na^+$, $K^+$, $Ca^{2+}$, $Mg^{2+}$) present in the transformation process is presented in Fig. 3. Concentrations of exchangeable $Na^+$ and $Ca^{2+}$ both constantly decreased and reached minimum values after 12 hr in the solid residue. After phosphogypsum treatment, a large significant amount of $Ca^{2+}$ in the solid phase was replaced by $Na^+$ to get into supernatant, which was the main reason for the decrease of $Ca^{2+}$ concentration. Therefore, the exchange reaction between $Na^{2+}$ of BR and $Ca^{2+}$
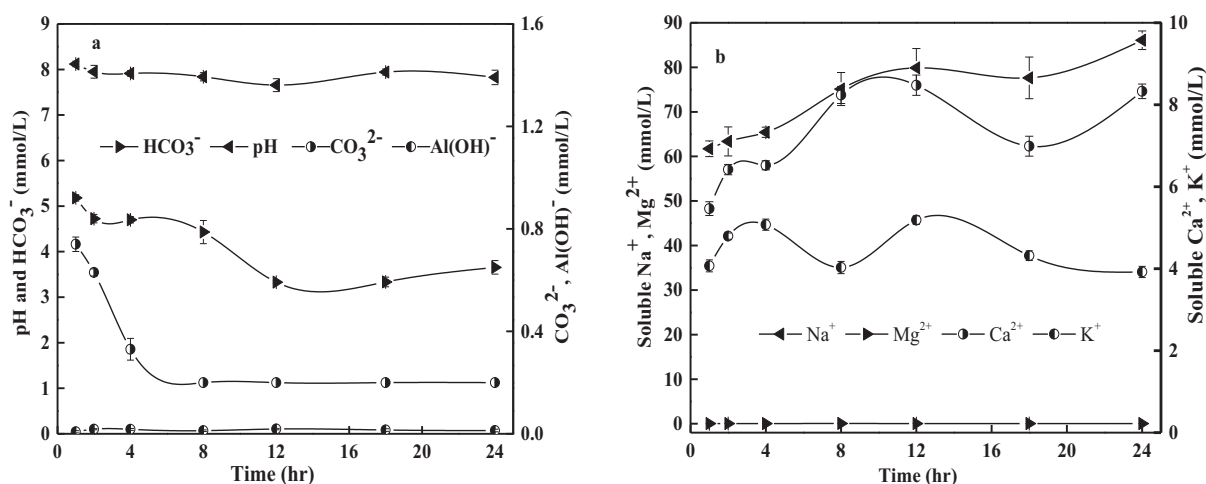


**Fig. 2 – Effect of reaction time on pH and soluble ion concentrations for supernatant with the addition of phosphogypsum to bauxite residue at 30°C and liquid/solid ratio of 2.**
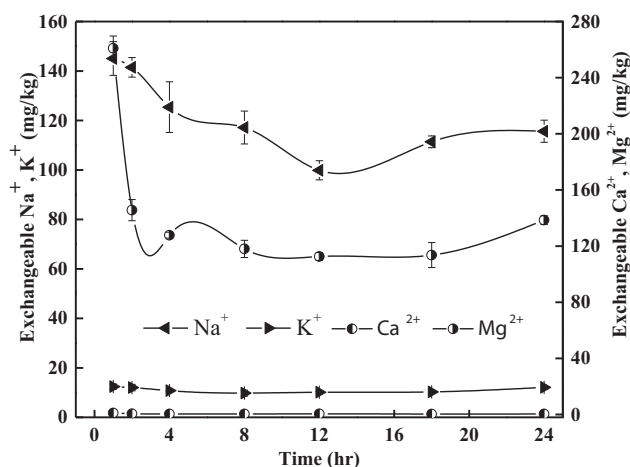
**Fig. 3 – Effect of reaction time on exchangeable cations of bauxite residue.**

in phosphogypsum was evidenced by both physical and chemical properties, particularly strong alkalinity in the short-term (Wong and Ho, 1991). But there were no significant difference around these treatment over 12 hr ($p < 0.05$), which was different from the study of Wong and Ho (1991) who reported that Na and alkalinity increased over time. Concentrations of K and Mg by the ammonium acetate extracted were not influenced by reaction time ($p > 0.05$).

Ultimately, the alkalinity of BR (pH, total alkalinity, $CO_3^{2-}$ and $HCO_3^-$) reduced to a minimum concentration after 12 hr. The change of reaction time mainly affected the concentration of alkaline ions.

### 2.3. Evaluation of bauxite residue dissolution

The lack of calcium in the leachate of BR is one of the reasons to limit reduction in pH. Phosphogypsum, as a solid waste, is available from the by-product of phosphate fertilizer industry. It usually contains both a large amount of calcium sulfate dihydrate and some phosphoric acid. The application of phosphogypsum is an effective method for alkaline and hazard amelioration in the bauxite residue. In conclusion, the reduction in pH, alkalinity and alkaline ions concentration may include three reaction mechanisms: (1) Neutralization: the phosphoric acid creates acid environment to neutralize the alkalinity and then generates $H_2O$ thus reducing the pH in the bauxite residue. (2) Precipitation: $OH^-$, $Al(OH)_4^-$ and $CO_3^{2-}$ in bauxite residue can precipitate calcium, which can generate $Ca(OH)_2$, $CaCO_3$ and $Ca_3Al_2(OH)_{12} \cdot CaCO_3 \cdot 5H_2O$. (3) Replacement: using waste phosphogypsum as a raw material for $Ca^{2+}$ source can replace the dissociative $Na^+$, significantly reducing the alkalinity of bauxite residue. Due to the existence of the above three reactions, it is apparent that phosphogypsum may regulate and control alkaline conditions to promote soil formation of bauxite residue.

### 2.4. Mineral phase and morphology characteristics

The mineral phases of the raw BR and BR reminded with phosphogypsum (2% phosphogypsum addition, L/S ratio 2

mL/g, temperature 30°C, and reaction time 12 hr) were analyzed by XRD (Fig. 4). The identified materials in the BR included hematite ($Fe_2O_3$), goethite (FeOOH), calcite ($CaCO_3$), hydrogarnet ($Ca_3Al_2(SiO_4)(OH)_8$)), cancrinite ($Na_6CaAl_6Si_6(CO_3)O_{24} \cdot 2H_2O$), Al hydroxides ($\alpha$-AlO(OH) and $Al(OH)_3$) and tricalcium aluminate (TCA, $Ca_3Al_2(OH)_{12}$) (Fig. 4a). Similar minerals have been reported for various bauxite residues worldwide (Kong et al., 2017b; Zhu et al., 2017).

It is noted that different production processes and digestion conditions, coupled with bauxite resources of diverse composition means that the ratio of the mineral phases in the BR invariably exhibited significant variation in quantity (Liao et al., 2015).

Due to the high digestion temperature (250°C) and higher level of CaO in the alumina production process, the chemical composition of BR from Pingguo alumina refinery contained a relatively high amount of ferrite. The ferrite mainly consisted of hematite ($Fe_2O_3$) and goethite (FeOOH), and the diffraction peak of $Fe_2O_3$ was the strongest among that of other minerals. Based on above results, the conversion of mineral phases was observed, which could offer a possibility to separate the goethitic alumina. For example aluminogoethite ($Fe_{(1 - x)}Al_xOOH(x = 0–0.33)$) may be converted to hematite (Suss et al., 2010) under such conditions. So, some suitable methods can be used to further recover iron and recycle the resources to reduce the hazard of bauxite residue.

Comparing with the phases in the original BR samples, the four mineral phases (hematite, calcite, hydrogarnet, cancrinite) existed in the residues after adding phosphogypsum. The peaks of cancrinite and hydrogarnet were strongest in all the alkaline minerals, indicating cancrinite and hydrogarnet were primary alkaline minerals in the transformation process (Fig. 4b).

Cancrinite can be dissolved under phosphogypsum slurry (Eq. (3)) and transformed into hydroxides (Zhang et al., 2011). The transformation mechanism for cancrinite is similar to acid condition (Eq. (12)), but the dissolution reaction is controlled by acid concentration. There existed a decomposition reaction of the cancrinite phase in BR, and the quantity of cancrinite decreased to 4.5 wt.% (Liao et al., 2015). When using
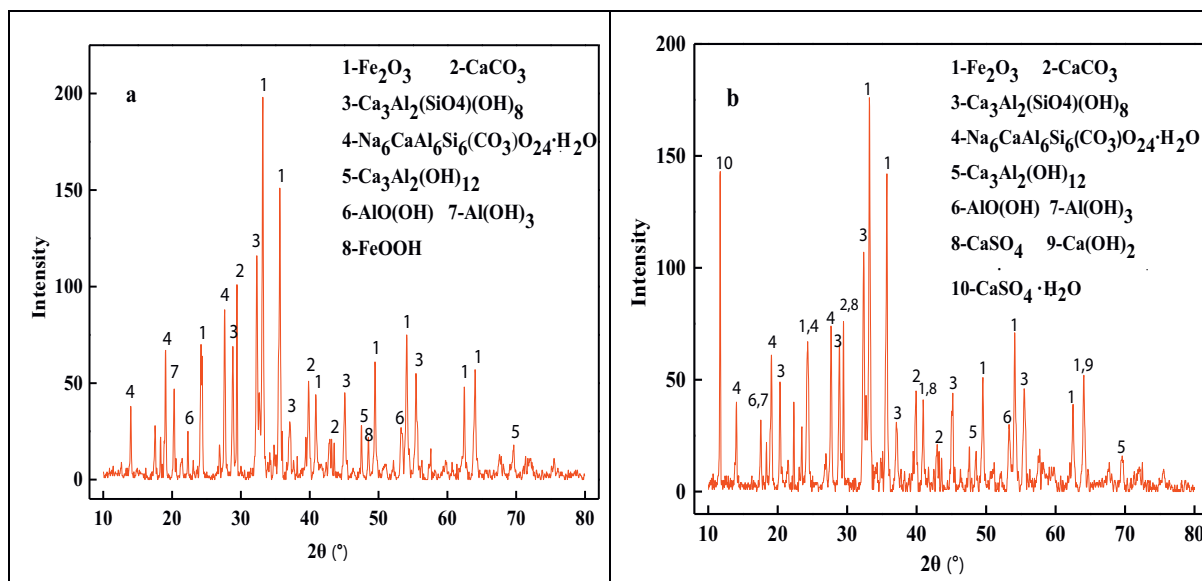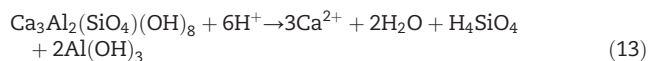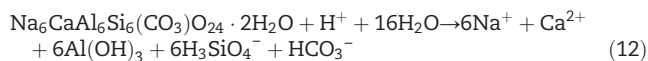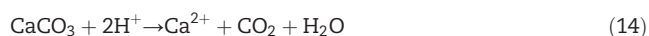
**Fig. 4 – X-ray diffraction patterns for bauxite residue and bauxite residue amended with phosphogypsum. Diffractograms were collected between 10 and 80° 2θ, with a step size of 1° at 60 sec per step. The strong peak of hydrogarnet was observed at 2θ = 32.3°.**

phosphogypsum to create acidic environment, the hydrogarnet can also be dissolved and precipitated to form gibbsite mineral phase (Couperthwaite et al., 2013) (Eq. (13)).

$$Na_6CaAl_6Si_6(CO_3)O_{24} \cdot 2H_2O + H^+ + 16H_2O \rightarrow 6Na^+ + Ca^{2+} + 6Al(OH)_3 + 6H_3SiO_4^- + HCO_3^- \tag{12}$$

$$Ca_3Al_2(SiO_4)(OH)_8 + 6H^+ \rightarrow 3Ca^{2+} + 2H_2O + H_4SiO_4 + 2Al(OH)_3 \tag{13}$$

Using a soluble calcium source, the alkalinity of BR can be precipitated in similar reactions to those with gypsum. There existed two equilibrium reactions during the process, including precipitation and dissolution reactions. Under acid environment (Lin et al., 2004), the mineral phase of calcium can be transformed (Eq. (14)). During acid transformation, calcite minerals are easy to be dissolved into the reaction solution (Kong et al., 2017b). Addition of phosphogypsum reduced the pH of mixed slurry to 8.05 and was conducive to form $CaCO_3$ (Eq. (15)). Phosphogypsum addition could bring $Ca^{2+}$ in solution, which precipitated excess soluble alkali to species such as tri-calcium aluminate, $Ca(OH)_2$ and $CaCO_3$ (Jones et al., 2012). Since the concentration of soluble carbonate was larger than that of $H^+$, the addition of phosphogypsum resulted in continually increasing calcite. It is possible that the calcium sources accelerated the precipitation of TCA (Eqs. (10)–(11)) to promote the alkaline reduction of bauxite residue. On the contrary, the calcium mineral (TCA) can be dissolved by acid transformation (Eq. (16)). These alkaline minerals, such as cancrinite, hydrogarnet, calcite and TCA, acting as alkaline storage, can buffer solution to a pH around 8.

$$CaCO_3 + 2H^+ \rightarrow Ca^{2+} + CO_2 + H_2O \tag{14}$$

$$Ca^{2+} + CO_3^{2-} \rightarrow CaCO_3 \tag{15}$$

$$Ca_3Al_2(OH)_{12} + 6H^+ \rightarrow 3Ca^{2+} + 2Al(OH)_3 + 6H_2O \tag{16}$$

The SEM image of bauxite residue (0.1–0.5 mm) illustrated particles were dispersed and of variable shapes (Fig. 5a). The raw sample included amorphous substances and these particles were of variable size. With the application of phosphogypsum, the loose particles disappeared and the aggregate particles were of uniform distribution (Fig. 5b). Adding phosphogypsum can promote the formation of stable macro-aggregates and these may form new particles (Zhu et al., 2016b, 2016e). Similar studies mentioned dispersion and micro-aggregation of BR by gypsum amendment, which provided forming conditions for a soil-like medium (Courtney and Mullen, 2009; Zhu et al., 2016d). Addition of gypsum and vermicompost on BR may directly affect aggregate size distribution and micromorphology, which can improve the aggregate structure and stability of BR (Zhu et al., 2017). Calcium and sodium contents varied significantly together with the change of mineral morphology. The total calcium content increased from 5.6% to 18.2%, whilst the total sodium content decreased from 6.8% to 2.4%. This behaviour was consistent with the results of exchangeable calcium and sodium.

## 3. Conclusions

This study confirmed that phosphogypsum regulated the alkaline characteristics of BR under the optimal condition of: water washing (L/S ratio 2, temperature 30°C and reaction time 24 hr); amount of phosphogypsum; and different reaction times which impacted the pH, EC, total alkalinity, soluble ions, exchange cation and morphology. Hydrogarnet,
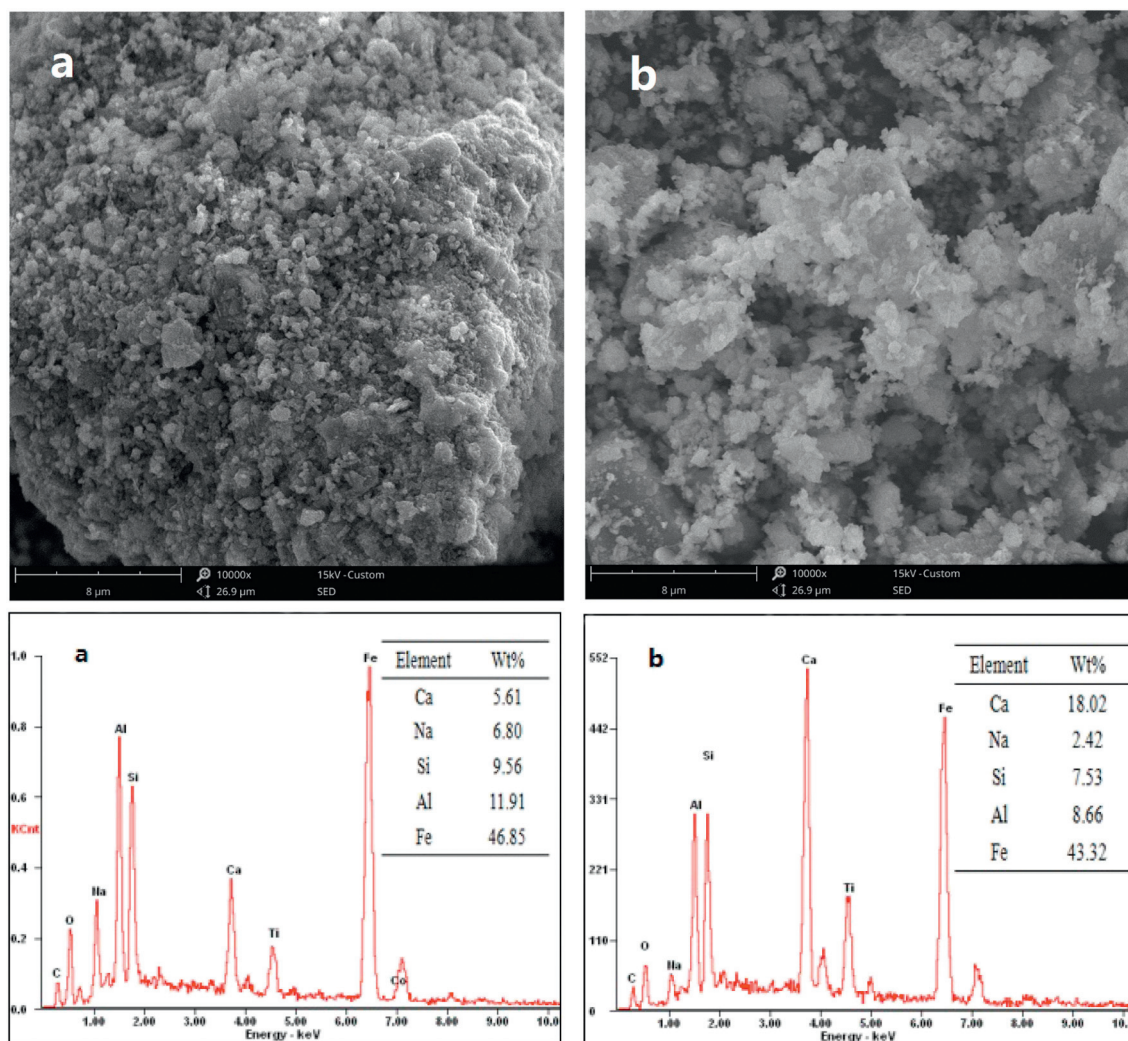
**Fig. 5 – Morphological structure and energy-dispersive X-ray analysis spectrum of solid residue obtained from macroaggregates (0.1–0.5 mm), the Fig. 5a was sample of bauxite residue and the Fig. 5b was sample of 2% phosphogypsum amendment.**

cancrinite and tri-calcium aluminate were the main alkaline phases. These alkaline minerals were able to facilitate alkaline storage and their dissolution in appropriate conditions could buffer the solution to a pH around 8. The optimal condition for the study was the addition of 2% phosphogypsum and a reaction time of 12 hr. Phosphogypsum addition promoted hydrogarnet and cancrinite transformation, whilst also promoting the exchange of sodium and calcium. With phosphogypsum application, pH and total alkalinity continually reduced, especially $CO_3^{2-}$ and $HCO_3^-$ concentrations. The total alkalinity and pH reduced from 50.8 to 4.1 mmol/L and 10.6 to 8.1, respectively; while the soluble $Na^+$ and $Ca^{2+}$ increased from 54.1 to 79.9 mmol/L, and 0.04 to 8.5 mmol/L, respectively. The exchangeable $Na^+$ and $Ca^{2+}$ in solid phase changed to 112 mg/kg and 259 mg/kg, respectively; so $Ca^{2+}$ became the dominant element in the solid phase. The phosphogypsum can change the loose granular structure of the BR and make it into a large aggregate structure. The reaction mechanism of phosphogypsum involved neutralization reaction, precipitation reaction and calcium sodium replacement co-precipitation reaction. The phosphogypsum transformation of BR is an important process and can be considered as a feasible way to treatment BRDAs. More importantly, it can achieve the purpose of "using waste treat waste" and reduce the risks of BRDAs, which is helpful to promote the soil formation' process of bauxite residue.

## Acknowledgments

## REFERENCES

Cánovas, C.R., Macías, F., Pérez López, R., Nieto, J.M., 2017a. Mobility of rare earth elements, yttrium and scandium from a phosphogypsum stack: environmental and economic implications. Sci. Total Environ. 618, 847–857.

Cánovas, C.R., Macías, F., Pérez-López, R., Basallote, M.D., Millán-Becerro, R., 2017b. Valorization of wastes from the fertilizer industry: current status and future trends. J. Clean. Prod. 174, 678–690.

Chen, Z., Wang, Y., Jiang, X., Fu, D., Xia, D., Wang, H., et al., 2017. Dual roles of AQDS as electron shuttles for microbes and dissolved organic matter involved in arsenic and iron mobilization in the arsenic-rich sediment. Sci. Total Environ. 574, 1684–1694.

Clark, M.W., Johnston, M., Reichelt-Brushett, A.J., 2015. Comparison of several different neutralisations to a bauxite refinery residue: potential effectiveness environmental ameliorants. Appl. Geochem. 56, 1–10.

Couperthwaite, S.J., Johnstone, D.W., Millar, G.J., Frost, R.L., 2013. Neutralization of acid sulfate solutions using bauxite refinery residues and its derivatives. Ind. Eng. Chem. Res. 52, 1388–1395.

Couperthwaite, S.J., Johnstone, D.W., Mullett, M.E., Taylor, K.J., Millar, G.J., 2014. Minimization of bauxite residue neutralization products using nanofiltered seawater. Ind. Eng. Chem. 53, 3787–3794.

Courtney, R.G., Harrington, T., 2012. Growth and nutrition of holcus lanatus, in bauxite residue amended with combinations of spent mushroom compost and gypsum. Land Degrad. Dev. 23 (2), 144–149.

Courtney, R.G., Kirwan, L., 2012. Gypsum amendment of alkaline bauxite residue — plant available aluminium and implications for grassland restoration. Ecol. Eng. 42 (5), 279–282.

Courtney, R.G., Mullen, G., 2009. Use of germination and seedling performance bioassays for assessing revegetation strategies on bauxite residue. Water Air Soil Pollut. 197 (1–4), 15–22.

Courtney, R.G., Timpson, J.P., 2005. Reclamation of fine fraction bauxite processing residue (red mud) amended with coarse fraction residue and gypsum. Water Air Soil Pollut. 164, 91–102.

Dilmore, R., Peng, L., Allen, D., Soong, Y., Hedges, S., Fu, J.K., et al., 2008. Sequestration of $CO_2$ in mixtures of bauxite residue and saline wastewater†. Energy Fuel 22, 1325–1333.

Gelencsér, A., Kováts, N., Turóczi, B., Rostási Hoffer, A., Imre, K., Nyirő-Kósa, I., et al., 2011. The red mud accident in Ajka (Hungary): characterization and potential health effects of fugitive dust. Environ. Sci. Technol. 45, 1608.

Gobran, G.R., Miyamoto, S., 1985. Dissolution rate of gypsum in aqueous salt solutions. Soil Sci. 140 (2), 89–93.

Higgins, D., Curtin, T., Pawlett, M., Courtney, R., 2016. The potential for constructed wetlands to treat alkaline bauxite-residue leachate: *Phragmites australis*, growth. Environ. Sci. Pollut. Res. 23, 24305–24315.

Higgins, D., Curtin, T., Courtney, R., 2017. Effectiveness of a constructed wetland for treating alkaline bauxite residue leachate: a 1-year field study. Environ. Sci. Pollut. Res. 24, 8516–8524.

Huang, Y., Chai, W., Han, G., Wang, W., Yang, S., Liu, J., 2016. A perspective of stepwise utilisation of Bayer red mud: step two —extracting and recovering Ti from Ti-enriched tailing with acid leaching and precipitate flotation. J. Hazard. Mater. 307, 318–327.

Johnston, M., Clark, M.W., Mcmahon, P., Ward, N., 2010. Alkalinity conversion of bauxite refinery residues by neutralization. J. Hazard. Mater. 182, 710–715.

Jones, B.E.H., Haynes, R.J., Phillips, I.R., 2012. Cation and anion leaching and growth of Acacia saligna, in bauxite residue sand amended with residue mud, poultry manure and phosphogypsum. Environ. Sci. Pollut. Res. 19 (3), 835–846.

Jones, B.E.H., Haynes, R.J., Phillips, I.R., 2015. Influence of amendments on acidification and leaching of Na from bauxite processing sand. Ecol. Eng. 84, 435–442.

Kinnarinen, T., Lubieniecki, B., Holliday, L., Helsto, J., Häkkinen, A., 2015. Recovery of sodium from bauxite residue by pressure filtration and cake washing. Int. J. Miner. Process. 141, 20–26.

Kirwan, L.J., Hartshorn, A., Mcmonagle, J.B., Fleming, L., Funnell, D., 2013. Chemistry of bauxite residue neutralisation and aspects to implementation. Int. J. Miner. Process. 119, 40–50.

Kong, X.F., Guo, Y., Xue, S.G., Hartley, W., Wu, C., Ye, Y.Z., et al., 2017a. Natural evolution of alkaline characteristics in bauxite residue. J. Clean. Prod. 143, 224–230.

Kong, X.F., Li, M., Xue, S.G., Hartley, W., Chen, C.R., Wu, C., et al., 2017b. Acid transformation of bauxite residue: conversion of its alkaline characteristics. J. Hazard. Mater. 324, 382–390.

Kong, X.F., Tian, T., Xue, S.G., Hartley, W., Huang, L., Wu, C., et al., 2018a. Development of alkaline electrochemical characteristics demonstrates soil formation in bauxite residue undergoing natural rehabilitation. Land Degrad. Dev. 29 (1), 58–67.

Kong, X.F., Jiang, X.X., Xue, S.G., Huang, L., Hartley, W., Wu, C., 2018b. Migration and distribution of salinity in bauxite residue during water leaching. Trans. Nonferrous Metals Soc. China 28 (3), 534–541.

Kopittke, P.M., Menzies, N.W., Fulton, I.M., 2005. Gypsum solubility in seawater, and its application to bauxite residue amelioration. Soil. Res. 42, 953–960.

Lee, Y.B., Bigham, J.M., Dick, W.A., Jones, F.S., Ramsier, C., 2007. Influence of soil pH and application rate on the oxidation of calcium sulfite derived from flue gas desulfurization. J. Environ. Qual. 36, 298–304.

Lehoux, A.P., Lockwood, C.L., Mayes, W.M., Stewart, D.I., Mortimer, R.J.G., Gruiz, K., et al., 2013. Gypsum addition to soils contaminated by red mud: implications for aluminium, arsenic, molybdenum and vanadium solubility. Environ. Geochem. Health 35, 643–656.

Li, X.F., Ye, Y.Z., Xue, S.G., Wu, C., Kong, X.F., Hartley, W., et al., 2018. Leaching optimization and dissolution behavior of alkaline anions in bauxite residue. Trans. Nonferrous Metals Soc. 28 (6) (in press).

Liao, C., Zeng, L., Shih, K., 2015. Quantitative X-ray diffraction (QXRD) analysis for revealing thermal transformations of red mud. Chemosphere 131, 171–177.

Lin, C., Maddocks, G., Lin, J., Lancaster, G., Chu, C., 2004. Acid neutralising capacity of two different bauxite residues (red mud) and their potential applications for treating acid sulfate water and soils. Aust. J. Soil Res. 42, 649.

Lockwood, C.L., Stewart, D.I., Mortimer, R.J.G., Mayes, W.M., Jarvis, A.P., Gruiz, K., et al., 2015. Leaching of copper and nickel in soil-water systems contaminated by bauxite residue (red mud) from Ajka, Hungary: the importance of soil organic matter. Environ. Sci. Pollut. Res. 22, 10800–10810.

Mayes, W.M., Burke, I.T., Gomes, H.I., Anton, Á.D., Molnár, M., Feigl, V., et al., 2016. Advances in understanding environmental risks of red mud after the Ajka spill, Hungary. J. Sustain. Metall. 2, 332–343.

Menzies, N.W., Fulton, I.M., Morrell, W.J., 2004. Seawater neutralization of alkaline bauxite residue and implications for revegetation. J. Environ. Qual. 33, 1877.

Newson, T., Dyer, T., Adam, C., Sharp, S., 2006. Effect of structure on the geotechnical properties of bauxite residue. J. Geotech. Geoenviron. 132, 143–151.

Paradis, M., Duchesne, J., Lamontagne, A., Isabel, D., 2007. Long-term neutralisation potential of red mud bauxite with brine amendment for the neutralisation of acidic mine tailings. Appl. Geochem. 22, 2326–2333.

Radomirovic, T., Smith, P., Southam, D., Tashi, S., Jones, F., 2013. Crystallization of sodalite particles under Bayer-type conditions. Hydrometallurgy 137, 84–91.

Rai, S., Wasewar, K.L., Lataye, D.H., Mukhopadhyay, J., Yoo, C.K., 2013. Feasibility of red mud neutralization with seawater using Taguchi's methodology. Int. J. Environ. Sci. Technol. 10, 305–314.

Santini, T.C., Hinz, C., Rate, A.W., Carter, C.M., Gilkes, R.J., 2011. *In situ* neutralisation of uncarbonated bauxite residue mud by

cross layer leaching with carbonated bauxite residue mud. J. Hazard. Mater. 194, 119–127.

Santini, T.C., Kerr, J.L., Warren, L.A., 2015. Microbially-driven strategies for bioremediation of bauxite residue. J. Hazard. Mater. 293, 131–157.

Singh, M., Garg, M., 2005. Study on anhydrite plaster from waste phosphogypsum for use in polymerised flooring composition. Constr. Build. Mater. 19, 25–29.

Suss, A., Fedyaev, A., Kuznetzova, N., Damaskin, A., Kuvyrkina, A., Panov, A., et al., 2010. Technology Solutions to Increase Alumina Recovery from Aluminogoethitic Bauxites. Tms. Light. Metals,  pp. 53–56.

Whittington, B.I., Fletcher, B.L., Talbot, C., 1998. The effect of reaction conditions on the composition of desilication product (DSP) formed under simulated Bayer conditions. Hydrometal-lurgy 49, 1–22.

Wong, J.W.C., Ho, G.E., 1991. Effects of gypsum and sewage sludge amendment on physical properties of fine bauxite refining residue. Soil Sci. 152 (5), 326–332.

Wu, C., Zou, Q., Xue, S.G., Pan, W.S., Yue, X., Hartley, W., et al., 2016. Effect of silicate on arsenic fractionation in soils and its accumulation in rice plants. Chemosphere 165, 478–486.

Xu, G., Ding, X., Kuruppu, M., Zhou, W., Biswas, W., 2018. Research and application of non-traditional chemical stabilizers on bauxite residue (red sand) dust control, a review. Sci. Total Environ. 1552, 616–617.

Xue, S.G., Zhu, F., Kong, X.F., Wu, C., Huang, L., Huang, N., et al., 2016a. A review of the characterization and revegetation of bauxite residues (Red mud). Environ. Sci. Pollut. Res. 23, 1120.

Xue, S.G., Kong, X.F., Zhu, F., Hartley, W., Li, X., Li, Y., 2016b. Proposal for management and alkalinity transformation of bauxite residue in China. Environ. Sci. Pollut. Res. 23, 12822–12834.

Xue, S.G., Wang, J., Wu, C., Li, S., Hartley, W., Wu, H., 2018. Physiological response of *Polygonum perfoliatum* L. following exposure to elevated manganese concentrations. Environ. Sci. Pollut. Res. 25 (1), 132–140.

Zhang, R., Zheng, S., Ma, S., Zhang, Y., 2011. Recovery of alumina and alkali in Bayer red mud by the formation of andradite-grossular hydrogarnet in hydrothermal process. J. Hazard. Mater. 189, 827–835.

Zhu, X., Li, W., Guan, X., 2015. An active dealkalization of red mud with roasting and water leaching. J. Hazard. Mater. 286, 85–91.

Zhu, F., Zhou, J.Y., Xue, S.G., Hartley, W., Wu, C., Guo, Y., 2016a. Aging of bauxite residue in association of regeneration: a comparison of methods to determine aggregate stability & erosion resistance. Ecol. Eng. 92, 47–54.

Zhu, F., Xue, S.G., Hartley, W., Huang, L., Wu, C., Li, X.F., 2016b. Novel predictors of soil genesis following natural weathering processes of bauxite residues. Environ. Sci. Pollut. Res. 23, 2856–2863.

Zhu, F., Liao, J.X., Xue, S.G., Hartley, W., Zou, Q., Wu, H., 2016c. Evaluation of aggregate microstructures following natural regeneration in bauxite residue as characterized by synchrotron-based X-ray micro-computed tomography. Sci. Total Environ. 573, 155–163.

Zhu, F., Huang, N., Xue, S.G., Hartley, W., Han, F.S., Li, Y.W., 2016d. Effects of binding materials on micro-aggregate size distribu-tion in bauxite residues. Environ. Sci. Pollut. Res. 23 (23), 23867–23875.

Zhu, F., Li, Y.B., Xue, S.G., Hartley, W., Wu, H., 2016e. Effects of iron-aluminium oxides and organic carbon on aggregate stability of bauxite residues. Environ. Sci. Pollut. Res. 23 (9), 9073–9081.

Zhu, F., Hou, J.T., Xue, S.G., Wu, C., Wang, Q.L., Hartley, W., 2017. Vermicompost and gypsum amendments improve aggregate formation in bauxite residue. Land Degrad. Dev. 28 (7), 2109–2120.

Zhu, F., Cheng, Q.Y., Xue, S.G., Li, C.X., Hartley, W., Wu, C., et al., 2018. Influence of natural regeneration on fractal features of residue microaggregates in bauxite residue disposal areas. Land Degrad. Dev. 29 (1), 138–149.